Multi-agent Modeling of Human Traffic Dynamics for Rapid Response to Public Emergency in Spatial Networks

Xiaoru Shi, Hankang Lee and Hui Yang*

Abstract—Public emergencies pose catastrophic casualties and financial losses in densely populated areas, rendering communities such as cities, towns, and universities particularly susceptible due to their intricate environments and high pedestrian traffic. While simulation analysis offers a flexible and cost-effective approach to evaluating evacuation procedures, conventional evacuation models are often limited to specific scenarios and communities, overlooking the diverse range of emergencies and evacuee behaviors. Thus, there is an urgent need for an evacuation model capable of capturing complex structures of communities and modeling evacuee responses to various emergencies. This paper presents a novel approach to simulating responsive evacuation behaviors for multiple emergency situations in public communities through spatial network modeling and multi-agent modeling. Leveraging a community network framework adaptable to different community layouts based on map data, the proposed model employs a multiagent approach to characterize responsive and decentralized evacuation decision-making. Experimental results show the model's efficacy in representing pedestrian flow and pedestrians' reactive behavior across various campuses based on real-world map data. Additionally, the case study highlights the potential of the proposed model to simulate pedestrian dynamics for a variety of heterogeneous emergencies. The proposed community evacuation model holds strong promise for evaluating evacuation policies and providing insights into resilient plans during public emergencies, thereby enhancing community safety.

Index Terms—Distributed decision, evacuation simulation, multi-agent modeling, network modeling, pedestrian flow.

I. INTRODUCTION

In recent years, the frequency of public incidents and natural disasters has increased, leading to substantial financial damage and casualties, especially in densely populated areas with complex structures and high pedestrian flow. These environments are particularly vulnerable due to their numerous buildings, intricate pathways, and high pedestrian traffic. Some public emergencies have necessitated evacuations, significantly impacting community mental health and disrupting regular operations [1]. Effective evacuation policies are essential to mitigate these disruptions. However, formulating such policies in large-scale communities, including cities, towns, and campuses, presents significant challenges due to their complex layouts and the unpredictable nature of emergencies. Factors like traffic flow, infrastructure constraints, and potential chaos during emergencies exacerbate

Xiaoru Shi is an undergraduate research student (REU), working with Hankang Lee (PhD student) and Hui Yang (Professor) in the Complex Systems, Monitoring, Modeling, and Control Lab, Harold and Inge Marcus Department of Industrial and Manufacturing Engineering, The Pennsylvania State University, University Park, PA 16802, USA. * Corresponding Author: huiyang@psu.edu

these challenges, rendering large-scale training impractical. Simulation modeling offers a valuable solution for evaluating evacuation policies, allowing the exploration of diverse scenarios without the risks and costs associated with physical drills. Nevertheless, conventional evacuation models often lack the versatility to assess evacuation processes across different environments. Therefore, it is crucial to develop a comprehensive model that captures the diverse structural characteristics and scenarios of heterogeneous communities for effective emergency planning and response.

Evacuation simulation models are inherently complex, incorporating non-linear pedestrian flow dynamics and the spread of hazards. Pedestrians, characterized by diverse demographic factors, exhibit different behaviors influenced by individual personality traits and travel purposes. The decision-making process of each pedestrian is not only influenced by their immediate surroundings and interactions with others but also distributed across the entire population, further complicating model development. Moreover, realworld emergencies often overlap, with one incident triggering subsequent emergencies. For instance, a severe fire may erupt following an explosion. In such scenarios, improper evacuation procedures can precipitate stampedes, exacerbating casualties. Hence, an evacuation model is urgently needed to account for pedestrian flow dynamics and multiple occurrences of diverse emergencies.

Building upon the complexities inherent in evacuation simulation models, this paper presents a novel approach to simulating responsive evacuation behaviors for multiple emergency situations in public communities through spatial network modeling and multi-agent modeling. The main contributions are as follows:

- We develop a community network model derived from real-world map data, comprehensively capturing structural features of diverse communities.
- 2) We design human agents to reflect pedestrians' responsive and decentralized decision-making, as well as hazard agents to represent the impact and spread of emergencies as each agent interacts within the model.

Simulation experiments on university campuses demonstrate the proposed model's effectiveness in representing pedestrian flow and reactive behavior across diverse settings. Furthermore, the case study results demonstrate the potential of the proposed model to evaluate key performance metrics for evacuation effectiveness in various environments.

The paper proceeds as follows: Section II introduces the background of evacuation simulation studies; Section III details the proposed methodology of the community evacuation

model; Section IV presents experimental design and results; and Section V concludes the research.

II. RESEARCH BACKGROUND

Simulation approaches have extensively assessed evacuation strategies, primarily focusing on indoor environments. Xu et al. developed a simulation model for evacuation during fires in a college building [2]. Zhou et al. introduced a force model to capture decentralized pedestrian behavior during subway station evacuations [3]. Zhang et al. proposed an event-based method to optimize building evacuation policies, integrating complex building structures into a queuing network [4]. Li et al. employed multi-agent reinforcement learning for real-time evacuation decision-making in complex buildings [5]. However, outdoor community environments pose distinct challenges due to their intricate path networks and high pedestrian flow. In large-scale emergencies affecting multiple buildings, evacuating from a single building may not ensure safety. Evacuees must navigate to shelters beyond hazardous areas, necessitating new modeling approaches. Previous studies on outdoor evacuations, such as those in public squares [6] and high school complexes [7], often relied on models specific to those environments, underscoring the need for more versatile solutions.

Leveraging geographical data from open sources like OpenStreetMap [8] enables the creation of network models that represent community topologies [9]. These models effectively illustrate complex system patterns, connectivity, and decentralized decision-making processes [10], [11]. For instance, spatial network models facilitate the analysis of virus spread and human mobility impacts [12], [13], while social contact networks assess COVID-19 transmission dynamics [14]. In manufacturing, networks of heterogeneous agents provide insights to optimize process flow [15]. Therefore, in this study, network modeling is developed to depict

TABLE I NOMENCLATURES

Notation	Definition
v_i	Node
s_{v_i}	Coordinate of the location of v_i
c_{v_i}	Capacity of v_i
$f_{v_i}(t)$	Pedestrian flow on v_i at t
e_{ij}	Edge between v_i and v_j
$l_{e_{ij}}$	Total length of e_{ij}
$c_{e_{i,i}}$	Capacity of e_{ij}
$f_{e_{ij}}(t)$	Pedestrian flow on e_{ij} at t
h_i	Hazard agent
$\zeta_{h_i}^{h_i}$	Time when h_i is emerged in the network
ζ_{h_i}	Lifespan of h_i
$s_{h_i}(t)$	Center of area impacted by h_i at t
$a_{h_i}(t)$	Radius of area impacted by h_i at t
\mathcal{V}_{h_i}	Movement speed of $s_{h_i}(t)$
$\mathcal{V}_{h_i}^s$	Expansion speed of $a_{h_i}(t)$
$\overline{p_i}$	Human agent
d_{p_i}	Destination node of p_i
$s_{p_i}(t)$	Location of p_i at t
$\mathcal{V}_{p_i}(t)$	Traveling velocity of p_i at t
$S_{p_i}(t)$	State of p_i at t
ϵ_{p_i}	Panic rate of p_i

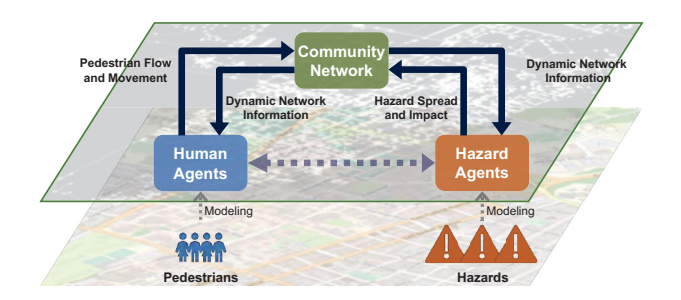


Fig. 1. Flowchart of the proposed multi-agent community network model and dynamic interactions between the components of the community network, human agents, and hazard agents.

community structures as pathways linking buildings and intersections, capturing pedestrian-environment interactions through networks of autonomous decision-making agents.

In evacuation modeling research, multi-agent approaches have proven essential for effectively capturing diverse pedestrian actions and interactions. For example, the agent-based model employing rule-based techniques was developed to simulate stadium evacuations during fires [16]. Luh et al. proposed a multi-agent modeling approach to scrutinize congestion effects and enhance evacuation strategies by simulating independent decision-making among pedestrians [17]. Furthermore, multi-agent modeling was employed to study psychological interactions, focusing on anxiety's impact on fire evacuations via virtual reality [18]. However, these studies often overlook the heterogeneous composition of pedestrian groups, influenced by demographic factors affecting behaviors such as panic likelihood and travel speed. Given the diversity and potential simultaneous or sequential emergencies in communities, it is crucial to develop a responsive evacuation model that accommodates various pedestrian behaviors and addresses cumulative emergency impacts.

III. METHODOLOGY

This section introduces a community evacuation model designed to simulate evacuation processes in large communities. The model captures pedestrian reactions to community networks and dynamic emergencies. As illustrated in Fig. 1, the proposed model consists of three components: 1) a community network representing pathways connecting buildings and intersections; 2) hazard agents simulating emergency spread and impact; and 3) human agents reflecting pedestrians' responsive behaviors to emergencies. Technical notations are outlined in Table I.

A. Community Network

The community map is structured into a multi-graph flow network denoted by G=(V,E), where V and E represent the sets of nodes and edges, respectively. Every community possesses a distinct geographical boundary, ensuring a finite node set V defined as:

$$V = \{v_i | i \in [1, n_v]\} \tag{1}$$

 $\begin{tabular}{ll} TABLE & II \\ STATES & OF THE & HUMAN & AGENT \\ \end{tabular}$

$S_{p_i}(t)$	Description
Normal	p_i is traveling unaffected.
Queuing	p_i is traveling but is in congestion.
Impacted	p_i is traveling but is impacted by hazards.
Arrival	p_i arrives at the destination without being impacted.
Survival	p_i arrives at the shelter after impacted by hazards.
Casualty	p_i becomes a casualty due to the effects of hazards.

where n_v denotes the number of nodes in the network. Each node v_i in the network is defined as follows:

$$v_i = (s_{v_i}, c_{v_i}, f_{v_i}(t)) \tag{2}$$

where s_{v_i} is the geographical coordinate of v_i , and c_{v_i} represents the pedestrian capacity estimated based on open-source community amenity data. Pedestrian flow $f_{v_i}(t)$ denotes the pedestrian flow at node v_i at time t.

Nodes are classified into buildings or non-buildings. Building nodes encompass community buildings, whereas non-building nodes represent intersections, parks, lawns, and parking lots. Evacuees can traverse these nodes unless impeded by hazards or congestion. During emergencies, routes redirect to shelters provided by community authorities. These shelters also serve as command centers for coordinating support and relief efforts.

In the community network, an edge represents a pathway between two nodes. The edge set E is defined as follows:

$$E = \{e_{ij} = (v_i, v_j) | v_i, v_j \in V^2, i \neq j\}$$
(3)

where each edge e_{ij} is denoted as follows:

$$e_{ij} = (l_{e_{ij}}, c_{e_{ij}}, f_{e_{ij}}(t))$$
 (4)

where $l_{e_{ij}}$ represents the practical distance for pedestrians traveling along e_{ij} . The edge length $l_{e_{ij}}$ is estimated as $l_{e_{ij}} = \lfloor l_{e_{ij}}^b \cdot w_{e_{ij}} \rfloor$ where $l_{e_{ij}}^b$ represents the Euclidean distance between v_i and v_j , and $w_{e_{ij}}$ is the degree of curvature of e_{ij} . The edge capacity $c_{e_{ij}}$ is formally defined as $c_{e_{ij}} = l_{e_{ij}} \cdot D_{\max}$ where D_{\max} is the maximum pedestrian volume sustainable per each unit length. Pedestrian flow $f_{e_{ij}}(t)$ reflects the number of pedestrians moving along e_{ij} at time t.

B. Hazard Agent

The set of hazard agents impacting the network is denoted as $H=\{h_i|1\leq i\leq \mathcal{H}_{\max}\}$, where \mathcal{H}_{\max} is the maximum number of emergencies during evacuation. Hazards are characterized by their causes and circular impact areas, with severity determined by both source and impact area characteristics. Each hazard agent h_i is defined by the following tuple of parameters:

$$h_{i} = \left(t_{0}^{h_{i}}, \zeta_{h_{i}}, \mathcal{V}_{h_{i}}, \mathcal{V}_{h_{i}}^{s}, s_{h_{i}}(t), a_{h_{i}}(t)\right) \tag{5}$$

where $t_0^{h_i}$ denotes the emergence time of h_i , and ζ_{h_i} represents the duration cessation. V_{h_i} and $V_{h_i}^s$ are the movement

and spread speeds within the impact area, respectively. Hazard agents contain two dynamic properties: $s_{h_i}(t)$ denotes the coordinate of the impact area center at time t, and $a_{h_i}(t)$ corresponds to the radius of the circular impact area.

C. Human Agent

Pedestrian flow is represented as a set of human agents denoted by $P = \{p_i | 1 \leq i \leq \mathcal{P}_{\max}\}$, where \mathcal{P}_{\max} denotes the maximum volume of pedestrian flow in the community. To capture the reactive behavior of pedestrians, each human agent p_i is defined as follows:

$$p_i = (d_{p_i}, s_{p_i}(t), \mathcal{V}_{p_i}(t), S_{p_i}(t), \epsilon_{p_i})$$
 (6)

where d_{p_i} denotes the destination of p_i , and $s_{p_i}(t)$ represents the current location of p_i at time t. Each human agent updates their traveling routes from $s_{p_i}(t)$ to d_{p_i} based on its observations of the community network and hazard occurrence. $\mathcal{V}_{p_i}(t)$ is the traveling speed of p_i at time t. The state of p_i is represented as $S_{p_i}(t)$, which is a set of six states: Normal, Queuing, Impacted, Arrival, Survival, and Casualty. Detailed descriptions of each state are outlined in Table II.

 $S_{p_i}(t)$ governs the decision-making process of p_i during the evacuation. The initial state of p_i is Normal. If a critical situation prevents p_i from continuing their current travel due to traffic congestion or inaccessibility to nodes or edges, $S_{p_i}(t)$ becomes Queuing. The Queuing state impedes the movement of p_i with a possible detour and reduced traveling speed. When p_i is influenced by a hazardous impact from an emergency, $S_{p_i}(t)$ turns to Impacted. Impacted p_i changes their destination to a nearby shelter and begins evacuation. p_i

Algorithm 1: Human-Network Interaction Algorithm

```
forall p_i \in P do
      if p_i is in panic then
                                          p_i randomly selects e_j \in E(v_k(t))
                                   else p_i is not in panic
                                          p_i re-routes
                                   Update s_{p_i}(t+1) based on \mathcal{V}_{p_i}(t)
                     else no congestion
                            Update s_{p_i}(t+1) based on \mathcal{V}_{p_i}(t)
              else p_i is located at e_w, for e_w \in E
                      \begin{array}{l} \text{if } f_{e_k}(t) \geq c_{e_k} \text{ then} \\ \downarrow S_{p_i}(t+1) \leftarrow \textit{Queuing and } \mathcal{V}_{p_i}(t) \leftarrow 0 \end{array} 
                     else no congestion
                            Update s_{p_i}(t+1) based on \mathcal{V}_{p_i}(t)
              end
      eld else p_i reaches d_{p_i} if S_{p_i}(t) = Normal then |S_{p_i}(t+1) \leftarrow Arrival else S_{p_i}(t) = Impacted |S_{p_i}^{\rm End} \leftarrow Survival end
      end
end
```

Algorithm 2: Human-Hazard Interaction Algorithm

can exit the model with one of three ending states: *Arrival*, *Survival*, or *Casualty*.

The panic rate ϵ_{p_i} represents the likelihood of panic when $S_{p_i}(t)$ becomes Impacted. The design of ϵ_{p_i} is based on the understanding that panic is positively related to the degree of uncertainty. When panicked, human agents deviate from optimal evacuation routes. The level of panic depends on the characteristics of pedestrians and the completeness of observation required for evacuation. These observations include knowledge of community structures and the presence of executive agencies.

During the evacuation, pedestrians rely on up-to-date observations of their immediate surroundings to make informed decisions. These observations include information about community structures and hazards. To reflect the process of collecting this information and making evacuation decisions, we design two algorithms: (1) Human-Network Interaction Algorithm and (2) Human-Hazard Interaction Algorithm.

Interactions between human agents and the community network are systematically modeled for each p_i at every time t, as outlined in Algorithm 1. These interactions are critical in shaping pedestrian flow, directly affecting the overall evacuation outcome. At each time t, the properties of each p_i are updated simultaneously, considering the current status of the community network and previous observations. This interaction mechanism ensures that the behavior of each human agent is dynamically influenced by evolving network conditions and observed information, thereby allowing a more realistic representation of pedestrian dynamics during the evacuation process.

Interactions between human agents and hazard agents are modeled for each p_i at each time t, as described in Algorithm 2. This algorithm details how each p_i actively observes hazard agents in their immediate vicinity while making limited observations of the community network and currently existing hazards. Additionally, this algorithm captures the detrimental effects of hazard agents on the survivability and decision-making of p_i during evacuation. The adverse effects of hazard agents on human agents manifest in two aspects. First, human agents initiate evacuation when they directly encounter or detect the negative effects of any hazard agents within a predetermined radius. Second, prolonged panic states lead to irrational behavior in which p_i persistently deviates from prescribed evacuation routes.

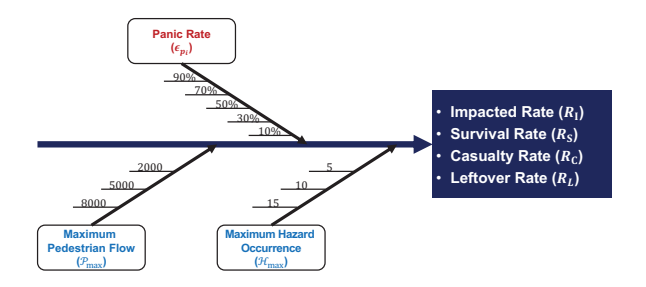


Fig. 2. Experimental design with three control factors and four performance metrics in the case study.

IV. EXPERIMENTAL DESIGN AND RESULTS

A. Experimental Design

The proposed evacuation model is evaluated in two steps. First, the community network model is verified through simulation experiments conducted in five representative municipal communities: the University Park campus of the Pennsylvania State University (PSU-UP), the Charlottesville campus of the University of Virginia (UVA-C), the Blacksburg campus of Virginia Tech (VT-B), Reading, PA (RA-PA), and King of Prussia, PA (KOP-PA). These communities were selected for their varying structural layouts and demographic characteristics, providing a comprehensive assessment of the model's applicability. Simulation outcomes provide a detailed analysis of network attributes and offer visualizations of pedestrian flow on community maps. These insights are crucial for understanding pedestrian navigation patterns and decision-making processes in both routine and emergency contexts.

Second, the multi-agent modeling approach is validated through a case study assessing evacuation effectiveness under varying panic levels. This study identifies three control factors to evaluate the impact of panic levels on evacuation outcomes, considering uncertainties in pedestrian flow and hazard occurrence, as shown in Fig. 2. The panic rate (ϵ_{p_i}) quantifies the negative impact on evacuation decisions due to imperfect observations. Pedestrian flow and hazard occurrence are regulated by two control factors: maximum pedestrian flow within the community $(\mathcal{P}_{\text{max}})$ and maximum

TABLE III
HUMAN AGENT GROUP PARAMETERS

Identity	Age Range	Speed (m)	Panic Rate (%)	portion (%)
Group 1	[18,25]	96	60	60
Group 2	[25,50]	84	50	20
Group 3	[40,60]	72	20	20

TABLE IV
HAZARD AGENT TYPE PARAMETERS

Type	Lifespan	Area as Radius	Expansion	Movement
Type	(minute)	(m)	Speed (m/s)	Speed (m/s)
Type 1	[130,170]	[150,200]	[25,35]	[30,42]
Type 2	[30,50]	[20,80]	[0,10]	[90,102]
Type 3	[120,170]	[200,400]	[100,120]	[102,204]

TABLE V
NETWORK STATISTICS

Network	Building Node	Non-building Node	Edge
	Count	Count	Count
PSU-UP	953	6,670	19,799
UVA-C	412	5,677	7,095
VT-B	445	6,511	6,929
RA-PA	473	2,068	16,432
KOP-PA	277	2,240	17,216

number of hazard occurrences $(\mathcal{H}_{\text{max}})$. Four performance measures are analyzed: impacted rate (R_{I}) , evacuation success rate (R_{S}) , casualty rate (R_{C}) , and leftover rate (R_{L}) . R_{I} defined as the ratio of affected pedestrians to the maximum pedestrian flow, $R_{\text{I}} = \frac{n_{\text{I}}}{\mathcal{P}_{\text{max}}}$, where n_{I} represents the number of pedestrians affected by any hazards. Other three metrics assess evacuation effectiveness as ratios to n_{I} : $R_{\text{S}} = \frac{n_{\text{S}}}{n_{\text{I}}}$, $R_{\text{C}} = \frac{n_{\text{C}}}{n_{\text{I}}}$, and $R_{\text{L}} = \frac{n_{\text{I}} - n_{\text{S}} - n_{\text{C}}}{n_{\text{I}}}$, where n_{S} and n_{C} denote the number of survivors and casualties, respectively. Diversity inherent in pedestrian behavior is modeled by defining three human agent groups, as outlined in Table III. These group parameters are designed to reflect variations in age, likelihood to panic, and travel speed. Additionally, three hazard types are characterized by diversified impacts and spreading behavior among hazards, as presented in Table IV.

B. Simulation Studies for Community Network Model

As presented in Table V, each municipal community is represented by a network characterized by varying numbers of building and non-building nodes, as well as edges. PSU-UP exhibits the most intricate network structure with 953 building nodes, 6,670 non-building nodes, and 19,799 edges. Across all communities studied, each community includes more than 200 buildings, over 2,000 intersections and open grounds, and around 6,500 edges. This underscores significant variability in the distribution of buildings, intersections, and pathways among communities, despite similarities in function, demographic profiles, and pedestrian patterns.

Community maps and corresponding spatial network representations of PSU-UP, UVA-C, VT-B, RA-PA, and KOP-PA are illustrated in Fig. 3. nodes are represented by white dots, and edges denote pathways. Despite each community having a unique network topology, the arrangement of buildings, intersections, and pathways follows a non-

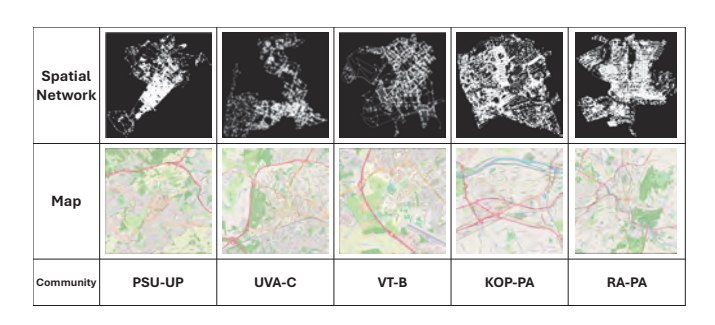


Fig. 3. Illustrations of spatial networks and campus maps of PSU-UP, UVA-C, VT-B, RA-PA, and KOP-PA.

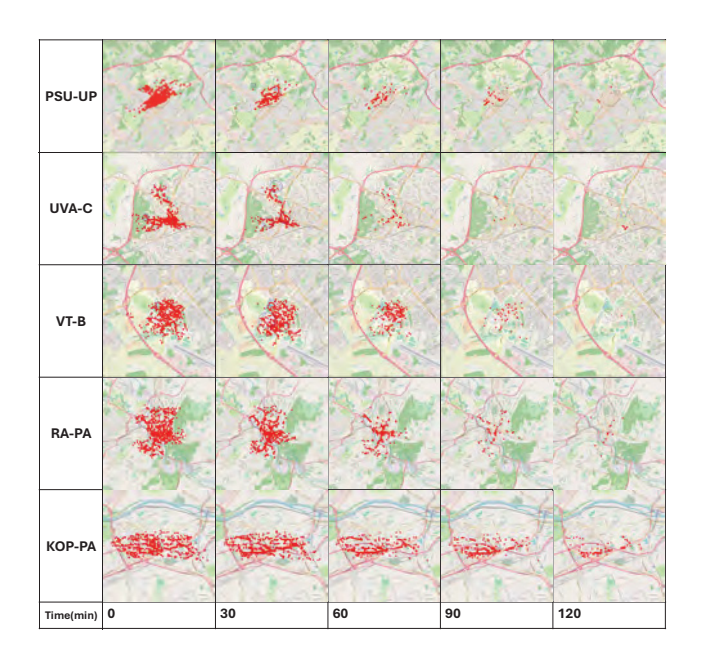


Fig. 4. Pedestrian flow and evacuation progress over time from 0 to 120 during evacuation on each campus.

linear pattern. The intricacy of communities emphasizes the necessity of employing network modeling to assess community-wide evacuation processes. The proposed community network model demonstrates flexibility and accuracy in representing the structural characteristics of each campus as a corresponding network when providing geographical indicators of the community.

In a scenario where $\mathcal{P}_{\text{max}}=2000$, $\mathcal{H}_{\text{max}}=5$, and $\epsilon_p=10\%$, the dynamic distribution of pedestrian flow on each campus is shown in Fig. 4, with red dots symbolize pedestrians. The observed distribution closely corresponds to structural features depicted by the campus's spatial network, validating the accuracy of the proposed community network model in predicting dynamic pedestrian flow patterns. Furthermore, as the simulation progresses, a noticeable decrease in pedestrian flow is evident on each campus. This decrease suggests the successful evacuation and effective route navigation of pedestrians while utilizing the flow-based network.

C. Case Study: Evacuation Performance across Panic Levels

The effect of \mathcal{P}_{max} and \mathcal{H}_{max} on the impacted rate (R_I) is depicted in Fig. 5. The analysis reveals that R_I exhibits no discernible correlation with \mathcal{P}_{max} but increases as the \mathcal{H}_{max} rises. For instance, when $\mathcal{H}_{max}=5$, the R_I values for each \mathcal{P}_{max} level are 34.3%, 27.5% and 34.4%. However, with \mathcal{H}_{max} increasing to 10, these values increase to 56.5%, 51.8% and 54.4%, respectively. Subsequently, with $\mathcal{H}_{max}=15$, the R_I values further increase to 68.4%, 64.4% and 66.2%, respectively. This trend suggests a higher frequency of emergencies affecting the community, resulting in an expansion of hazardous impact areas within the community network. Consequently, the cumulative impact areas expand, leading to an increased number of affected nodes and edges within

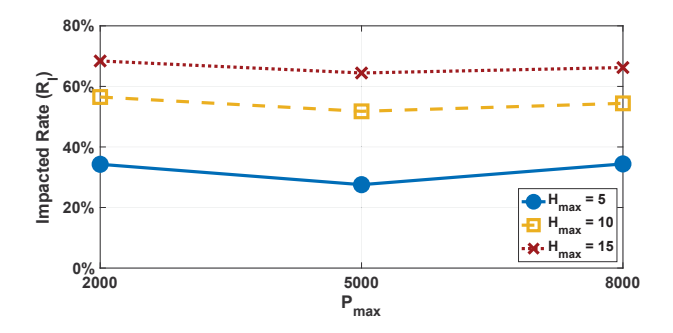


Fig. 5. Impacted rate of pedestrians according to maximum pedestrian flow and maximum number of hazard occurrences.

the network. Given that pedestrians are spatially distributed within the community network based on a fixed \mathcal{P}_{max} level, the surge in \mathcal{H}_{max} results in a pronounced escalation in the number of pedestrians impacted by hazards.

The degree of background panic rate influences the evacuation effectiveness as illustrated in Fig. 6. First, a distinct negative relationship is observed between ϵ_p and R_S . Specifically, when $\epsilon_p = 10\%$, 96.6% of evacuees successfully reach shelters within 120 minutes. However, a rise in ϵ_p exacerbates the panic level among impacted pedestrians, leading to confusion in their evacuation decision-making process. This trend is supported by the decrease in $R_{\rm S}$ observed at higher ϵ_p levels. For example, when the ϵ_p parameters are set to 50% and 90%, only 88.3%, and 64.6% of the impacted pedestrians, respectively, manage to safely evacuate. Furthermore, another observation is the increase in the probability of casualties among impacted pedestrians as ϵ_p rises. A lower value of ϵ_p indicates that pedestrians possess most of the information necessitated for successful evacuation. In particular, when ϵ_p is set to 10%, 2.5% of affected pedestrians become casualties. On the other hand, R_C increases to 7.2% and 13.3% when $\epsilon_p = 50\%$ and $\epsilon_p = 90\%$, respectively.

Moreover, an indication of the decreased rationality concerning evacuation decisions emerges in the context of $R_{\rm L}$ as ϵ_p increases. Given the assumption that panic states are irreversible, panicked pedestrians make minimal progress toward nearby shelters. These individuals are unlikely to reach any definitive end states, such as casualties or successful evacuations, as they persist in following random paths once panic occurs. Thus, a higher ϵ_p correlates with a greater likelihood of pedestrians remaining within the network after 120 minutes. For example, when $\epsilon_p = 10\%$, R_L remains below 1%. However, if ϵ_p values become 70% and 90%, the corresponding $R_{\rm L}$ surges to 9.7% and 22.1%, respectively. It is noteworthy that as ϵ_p rises, $R_{\rm L}$ increases at a faster rate than $R_{\rm C}$. The reason is the congestion caused by the concentration of panicked evacuees wandering aimlessly around surrounding areas without proper evacuation progress.

Holding all other control factors constant, a rise in \mathcal{P}_{max} proportionally increases n_{I} , n_{S} , and n_{C} , while having minimal impact on R_{C} , R_{L} , and R_{S} . Similarly, an increase in \mathcal{H}_{max} results in a higher n_{I} , which consequently elevates

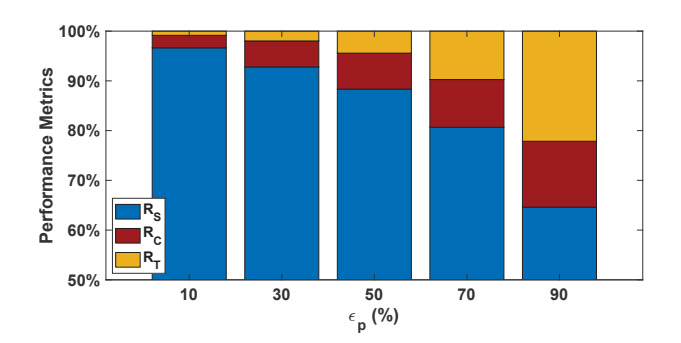


Fig. 6. Proportional performance metrics $(R_{\rm S},\,R_{\rm C},\,{\rm and}\,R_{\rm L})$ with respect to background panic rate.

 $R_{\rm I}$, given a fixed pedestrian population. However, without altering the panic rate ϵ_p , rasing $\mathcal{H}_{\rm max}$ does not significantly influence $R_{\rm L}$, $R_{\rm C}$, or $R_{\rm S}$. Additionally, increasing $\mathcal{P}_{\rm max}$ requires substantial computational resources for simulation experiments due to the increased interactions among human agents and hazard agents. Within a Python 3.7 simulation environment running on a system with 16 GB of RAM and an Apple M1 Pro chip (8-core CPU, 14-core GPU), increasing $\mathcal{P}_{\rm max}$ from 2,000 to 8,000 extends the duration of a single simulation run from 2.5 hours to 22 hours, while keeping all other control factors constant. Despite this increased computational demand, the enhanced interactions provide decision-makers with valuable insights, particularly in monitoring pedestrian flow and identifying areas susceptible to congestion and potential stampedes.

D. Discussion

The proposed community evacuation model provides a comprehensive framework for evaluating evacuation processes in diverse outdoor and municipal environments characterized by complex and dynamic pedestrian flow. However, the current model has two limitations: it assumes that panic is irreversible and that panicking pedestrians choose paths randomly at nodes. These assumptions do not fully reflect the nuanced behaviors observed during real-world evacuations. Future research should aim to refine these assumptions to more accurately capture the actual responses of pedestrians during emergencies.

When integrated into emergency response systems, the model is invaluable for proactively evaluating and optimizing evacuation strategies before emergencies occur. Effective deployment involves the strategic allocations of resources, such as shelters, emergency responders, and relief personnel, to maximize evacuee survival rates. By visualizing pedestrian flow, decision-makers can identify high-density areas and adjust disaster relief efforts accordingly. Future enhancements may include additional agent types, such as firefighters and trained volunteers, to more accurately represent evacuees and response activities.

Incorporating real-world map data into network modeling allows the simulation of diverse community layouts, enhancing the model's ability to reflect various structural characteristics. The multi-agent modeling approach further improves the representation of individual decision-making processes among evacuees and hazards, ensuring autonomous operation and efficient computational performance. To advance the model's capability in simulating reactive evacuee behaviors during panic, future research will explore the application of foundational theories of human behavior, such as social force models. Additionally, modeling irrational behaviors triggered by evolving hazards could be refined by applying probabilistic approaches like Markov Decision Processes.

V. CONCLUSIONS

In this paper, we presented the community evacuation model designed to evaluate evacuation protocols within municipal communities, achieved by simulating the responsive behavior of evacuating pedestrians for multiple emergencies through network modeling and multi-agent modeling. This methodology furnishes novel features that contribute to efficacy and adaptability through the integration of the following modeling methods:

- Community spatial network: The methodology incorporates network modeling, which represents the structural properties of communities through a network of interconnected buildings, intersections, and pathways. The proposed network model provides an effective mechanism for modeling diverse community environments and simulating dynamic pedestrian flow by leveraging real-world map data.
- 2) Human and hazard agents: Multi-agent modeling adequately captures multifaceted characteristics and dynamics inherent in pedestrian behavior and emergency spread. Hazard agents are designed to encapsulate the dynamic propagation and impact of public emergencies. Human agents reflect pedestrian behavior by embodying their attributes and decision-making processes in response to emergency scenarios, representing pedestrian flow.

The proposed modeling methodology is validated through an experimental study with two phases. First, the community network model effectively represented pedestrian flow within spatial networks of three university campuses. Second, experimental outcomes of the case study evaluating evacuation performance across different panic levels showed that the proposed multi-agent modeling method proficiently reflects the intricate dynamics of evacuation processes. This community evacuation model is strongly promised to enhance lifesaving measures during community-wise exigent situations with an approach to simulate and provide decision support to both evacuation procedures and subsequent actions.

ACKNOWLEDGEMENT

This paper is based upon research studies supported by the U.S. National Science Foundation under award number IIS-2302834. Any opinions, findings, or conclusions found in this paper are those of the authors and do not necessarily reflect the views of the sponsor.

REFERENCES

- M. A. Tkachuck, S. E. Schulenberg, and E. C. Lair, "Natural disaster preparedness in college students: Implications for institutions of higher learning," *Journal of American College Health*, vol. 66, no. 4, pp. 269– 279, 2018.
- [2] M. Xu and D. Peng, "Pyrosim-based numerical simulation of fire safety and evacuation behaviour of college buildings," *International Journal of Safety and Security Engineering*, vol. 10, no. 2, pp. 293– 299, 2020.
- [3] R. Zhou, Y. Cui, Y. Wang, and J. Jiang, "A modified social force model with different categories of pedestrians for subway station evacuation," *Tunnelling and Underground Space Technology*, vol. 110, p. 103837, 2021.
- [4] Y. Zhang, Z. Xu, J. Wu, and X. Guan, "An event-based optimization method for building evacuation with queuing network model," in 2021 IEEE 17th International Conference on Automation Science and Engineering (CASE). IEEE, 2021, pp. 1961–1966.
- [5] X. Li, H. Liu, J. Li, and Y. Li, "Deep deterministic policy gradient algorithm for crowd-evacuation path planning," *Computers & Industrial Engineering*, vol. 161, p. 107621, 2021.
- [6] S. Liu, J. Liu, and W. Wei, "Simulation of crowd evacuation behaviour in outdoor public places: A model based on shanghai stampede," *International Journal of Simulation Modelling*, vol. 18, no. 1, pp. 86– 99, 2019
- [7] P. Lu, D. Chen, Y. Li, X. Wang, and S. Yu, "Agent-based model of mass campus shooting: Comparing hiding and moving of civilians," *IEEE Transactions on Computational Social Systems*, 2022.
- [8] M. Haklay and P. Weber, "Openstreetmap: User-generated street maps," *IEEE Pervasive Computing*, vol. 7, no. 4, pp. 12–18, 2008.
- [9] G. Boeing, "Osmnx: New methods for acquiring, constructing, analyzing, and visualizing complex street networks," Computers, Environment and Urban Systems, vol. 65, pp. 126–139, 2017.
- [10] H. Yang, C. Kan, A. Krall, and D. Finke, "Network modeling and internet of things for smart and connected health systems—a case study for smart heart health monitoring and management," *IISE Transactions on Healthcare Systems Engineering*, vol. 10, no. 3, pp. 159–171, 2020.
- [11] C. Kan and H. Yang, "Dynamic network monitoring and control of in situ image profiles from ultraprecision machining and biomanufacturing processes," *Quality and Reliability Engineering International*, vol. 33, no. 8, pp. 2003–2022, 2017.
- [12] S. Zhang and H. Yang, "Spatial modeling and analysis of human traffic and infectious virus spread in community networks," in 2021 43rd Annual International Conference of the IEEE Engineering in Medicine & Biology Society (EMBC). IEEE, 2021, pp. 2286–2289.
- [13] H. Yang, S. Zhang, R. Liu, A. Krall, Y. Wang, M. Ventura, and C. Deflitch, "Epidemic informatics and control: A review from system informatics to epidemic response and risk management in public health," in AI and Analytics for Public Health, H. Yang, R. Qiu, and W. Chen, Eds. Springer, 2022, pp. 1–58.
- [14] T. Luo, Z. Cao, Y. Wang, D. Zeng, and Q. Zhang, "Role of asymptomatic covid-19 cases in viral transmission: Findings from a hierarchical community contact network model," *IEEE Transactions* on Automation Science and Engineering, vol. 19, no. 2, pp. 576–585, 2021.
- [15] H. Lee and H. Yang, "Digital twinning and optimization of manufacturing process flows," *Journal of Manufacturing Science and Engineering*, vol. 145, no. 11, 2023.
- [16] J. Shi, A. Ren, and C. Chen, "Agent-based evacuation model of large public buildings under fire conditions," *Automation in Construction*, vol. 18, no. 3, pp. 338–347, 2009.
- [17] P. B. Luh, C. T. Wilkie, S.-C. Chang, K. L. Marsh, and N. Olderman, "Modeling and optimization of building emergency evacuation considering blocking effects on crowd movement," *IEEE Transactions on Automation Science and Engineering*, vol. 9, no. 4, pp. 687–700, 2012.
- [18] X. Lu, P. B. Luh, A. Tucker, T. Gifford, R. S. Astur, and N. Olderman, "Impacts of anxiety in building fire and smoke evacuation: modeling and validation," *IEEE Robotics and Automation Letters*, vol. 2, no. 1, pp. 255–260, 2016.